Tuning the atomic and domain structure of epitaxial films of multiferroic $BiFeO_3$

C. J. M. Daumont,[1] S. Farokhipoor,[1] A. Ferri,[1] J. C. Wojdeł,[2] Jorge Íñiguez,[2] B. J. Kooi,[1] and B. Noheda[1,*]
[1]*Zernike Institute for Advanced Materials, University of Groningen, Groningen 9747AG, The Netherlands*
[2]*Institut de Ciència de Materials de Barcelona (CSIC), Campus UAB, 08193 Bellaterra, Spain*
(Received 24 March 2010; published 15 April 2010)

Recent works have shown that the domain walls of room-temperature multiferroic $BiFeO_3$ (BFO) thin films can display distinct and promising functionalities. It is thus important to understand the mechanisms underlying domain formation in these films. High-resolution x-ray diffraction and piezoforce microscopy, combined with first-principles simulations, have allowed us to characterize both the atomic and domain structure of BFO films grown under compressive strain on (001)-$SrTiO_3$, as a function of thickness. The clamping of the substrate has been observed to exist in two different regimes: ultrathin, $d<18$ nm, and thin, $d>18$ nm. When this is taken into account in the calculations, an excellent agreement between the predicted and observed lattice parameters is shown. We derive a twinning model that describes the experimental observations and could explain why the 71° domain walls are the only ones showing insulating character. This understanding of the exact mechanism for domain formation provides us with a new degree of freedom to control the structure and, thus, the properties of $BiFeO_3$ thin films.

DOI: 10.1103/PhysRevB.81.144115 PACS number(s): 77.55.Nv, 71.15.Mb, 77.55.Px, 77.80.Dj

I. INTRODUCTION

Magnetoelectric multiferroics exhibit coupled electric and magnetic orders, which might lead to a variety of novel devices that would benefit from the fact that the magnetization (polarization) of these materials can be controlled by means of an electric (magnetic) field.[1] For practical devices, multiferroics are preferred in thin film form. Moreover, the strain induced by the mismatch between the film and the substrate lattice parameters can sometimes be used to tune the film properties with respect to the bulk.[2]

Bismuth Ferrite, $BiFeO_3$ (BFO), is one of the few multiferroics that orders above 300 K and, thus, one of the most promising ones.[3] The ferroelectric properties of BFO are very robust and it displays record polarization values of about 100 $\mu C/cm^2$. Since the ground state of bulk BFO is rhombohedral (space group $R3c$), symmetry arguments suggest that the thin films grown on cubic substrates under compressive epitaxial strain should be monoclinic (space group Cm or Cc, depending on whether the O_6 octahedra rotations are clamped by the substrate or not, respectively). Indeed, several authors[4–7] have reported a monoclinic unit cell that is similar to that of strong piezoelectric $PbZr_{1-x}Ti_xO_3$ (PZT) with $x \approx 0.5$.[8] The proposed link between the strong piezoelectricity and the symmetry of the unit cell,[9] which allows the polarization to rotate, adds to the interest of BFO films.[7]

Beyond their intrinsic properties, BFO films are currently receiving renewed attention because of the novel functionalities observed to occur at domain walls (DWs). Indeed, recent works have shown that some BFO DWs are highly conductive,[10] and that the DW density controls the magnitude of the (exchange bias) coupling between BFO and other (metallic) layers in complex heterostructures.[11] It is thus of prime importance to achieve control of the domain structures and understand their formation. In contrast, it is striking to note the scarcity, and lack of agreement, of experimental information on the atomic structure of the films and its evolution with thickness.[4,6,12] Indeed, we believe that a complete picture of the structure of these films does not exist yet.

We have grown BFO thin films on $SrRuO_3$-buffered $SrTiO_3$ (STO) substrates and followed the unit-cell distortion as a function of thickness during the first stages of strain relaxation. Our c/a ratios are consistent with those in Ref. 6. Additionally, we have been able to resolve the monoclinic distortion and measure the evolution of the full unit cell. The comparison of the experimental results with several structural models simulated *ab initio* allowed us to resolve the monoclinic space group (Cc) and atomic structure, as well as the polarization direction.

II. METHODOLOGY

Several (001)-oriented BFO thin films with thickness ranging from 12 to 87 nm were grown on atomically flat, TiO_2-terminated (001)-STO substrates with low miscut angle (0.1°). Conductive layers of $SrRuO_3$ with a thickness of 5 nm were deposited in between the substrate and the BFO layer. The BFO films were grown by pulsed laser deposition (PLD), assisted by reflective high-energy electron diffraction, using a pulsed KrF excimer laser ($\lambda = 248$ nm) with a repetition rate of 0.5 Hz. The deposition was performed at 670 °C in an oxygen pressure of 0.3 mbar. After deposition, the films were cooled down slowly to room temperature under an oxygen pressure of 100 mbar. The local ferroelectric response of the films was characterized by means of piezoforce microscopy (PFM),[13] using a Dimension V (VEECO) microscope with conducting tip and no top electrode. All the films showed ferroelectric response with the polarization vector pointing toward the substrate and all could be switched with the electric field applied between the bottom $SrRuO_3$ electrode and the tip. Both, the in-plane and the out-of-plane piezoelectric responses have been imaged.

The evolution of the crystallographic distortion with thickness was investigated by mapping the reciprocal space using x-ray diffraction (XRD) from laboratory sources, for mapping out-of-plane scattering planes, and synchrotron

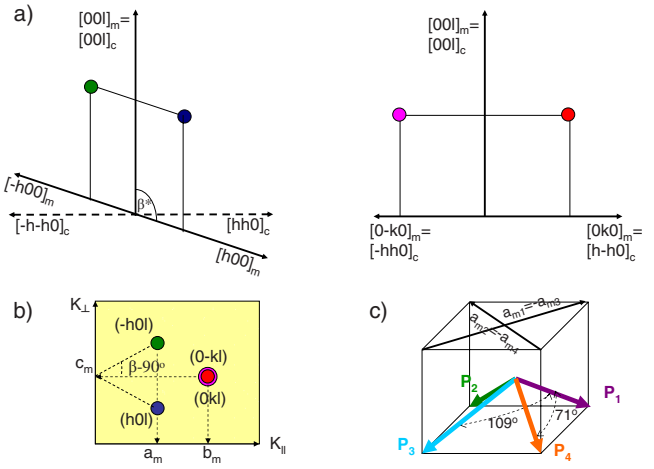

FIG. 1. (Color online) (a) Monoclinic domains in BFO thin films under compressive strain, in the $(h0l)_m$ (left) and $(0kl)_m$ (right) scattering planes. (b) Diffraction map around the $(h0l)_m$ reflections when all four domains are present. (c) Directions of the polarization and the monoclinic lattice parameter, a_m, for the four down polarized domains. In our films, the polarization direction has been calculated to be rotated 5° away from the [111] toward the [001] direction (see text).

sources (W1 beamline at HASYLAB-DESY) for mapping the in-plane scattering planes. Due to the epitaxy, which fixes the [001] direction in reciprocal space to be perpendicular to the substrate surface, the possible monoclinic domains with polarization pointing down are reduced to four and the reciprocal space maps are significantly simplified (similar to the case of a crystal under an electric field[14]). In particular, if all domains are present, looking at the areas around the substrate $(hhl)_c$, which corresponds to the $(h0l)_m$ reflection in the monoclinic structure,[15] one can extract the three lattice parameters and the monoclinic angle, as sketched in Fig. 1.

Our first-principles simulations were based on the so-called "LDA+U" approach to density-functional theory, the technical details being exactly as those in Ref. 16. We checked that our calculation conditions were well converged and reproduced basic results for BFO in the literature (as, e.g., the related ones in Ref. 17). It has been shown that ferroelectric thin films can be successfully studied by simulating the corresponding bulk material subject to elastic boundary conditions that mimic the epitaxial constraints imposed by the substrate. In this work we extended such an approach to make a distinction between the cases of *ultrathin* ("uth") and *thin* ("th") films, for which we consider different elastic constraints. More precisely, in the "uth" case we assumed the film is strongly clamped by the substrate, and impose $a_{pc}=b_{pc}=a_{\mathrm{STO}}$ and $\alpha_{pc}=\beta_{pc}=\gamma_{pc}=90°$. Note that a_{STO} is the lattice parameter of the $SrTiO_3$ substrate, which imposes an epitaxial strain of about −1.5% to the BFO film. In contrast, in the "th" case we only imposed that the in-plane area be constrained to be a_{STO}^2. This allowed us to model the ultrathin-to-thin transition evidenced by the experimental results (see the discussion of Fig. 3 below). Finally, in our simulations we considered two structural models, with and without rotations of the O_6 octahedra, which correspond, respectively, to the *Cc* and *Cm* space groups.

III. RESULTS AND DISCUSSION

Typical reciprocal space maps (RSMs) around the $(113)_c$ STO substrate reflections for ultrathin (<18 nm) and thin (>18 nm) films are shown on Fig. 2(a). The RSMs of the thinnest BFO films display a broad $(113)_c$ peak (using the pseudocubic notation), at the same k_{par} (in-plane component of the scattering vector) of the substrate, showing that they are fully coherent with the substrate. The FWHM of these films agrees with what is expected for their thicknesses. There is thus no indication of unresolved splitting. Therefore, the films appear as fully coherent and tetragonal and any possible deviation from the tetragonal symmetry that might exist should be due to distortions of the oxygen octahedra.

The RSMs of thicker films display a splitting of the $(113)_{pc}$ BFO peak, as expected (see Fig. 1). The monoclinic lattice parameters extracted from these patterns are plotted in Fig. 3. Interestingly, c_m shows no changes with increasing thickness. This is in agreement with the report by Kim *et al.*,[6] who showed that the lattice parameters of the strained films are constant below ~100 nm, a puzzling and unexplained result. However, for thickness above 18 nm we observe a splitting of the in-plane parameter values and a $\beta \neq 90°$, characteristic of a monoclinic distortion. Figure 3 reveals a gradual increase in the monoclinic distortion a_m-b_m with thickness. In addition, grazing incidence XRD has shown that the in-plane pseudocubic angle, γ_{pc} is, indeed, different from the out-of-plane angle β, and that such a difference decreases with increasing thickness ($\gamma_{pc}=\beta$ in the relaxed structure). Interestingly, the deviation of a_m and b_m from the value of $2\times d_{(110)}$ (i.e., the fully coherent case) is symmetric. As a consequence, the in-plane area of the cell remains essentially constant, which seems consistent with the fact that the out-of-plane lattice parameter is unchanged.

First-principles simulations allowed us to ratify these results and gain further insight into the atomic structure of the BFO films. Our results clearly indicate that the BFO films present significant O_6 rotations and thus the *Cc* space group. Indeed, when allowing for O_6 rotations we computed $a_m^{\mathrm{th}}/a_m^{\mathrm{uth}}=1.0012$ and $b_m^{\mathrm{th}}/b_m^{\mathrm{uth}}=0.9989$ for the splitting of in-plane lattice parameters, in reasonable agreement with the experimental values of 1.0018 and 0.9989 derived from Fig. 3 using the data points immediately adjacent to the ultrathin-to-thin transition. In contrast, when the O_6 tiltings are clamped in the simulations, we obtained $a_m^{\mathrm{th}}/a_m^{\mathrm{uth}}=1.0044$ and $b_m^{\mathrm{th}}/b_m^{\mathrm{uth}}=0.9956$. The c_{pc}/a_{pc} ratios follow the same pattern: the value computed with (without) O_6 tiltings is about 1.03 (1.09), to be compared with the experimental result of approximately 1.04, which strongly suggests that even in the thinnest films the O_6 rotations are not fully clamped by the substrate. These results provide a justification to first-principles studies of monoclinic BFO films in which a structural model with O_6 rotations is adopted (see, e.g., Ref. 17). Additionally, for the calculated monoclinic angle we obtained $\beta=90.1°$, which seems compatible with our experimental results, and we computed $c_{pc}^{\mathrm{th}}/c_{pc}^{\mathrm{uth}}=1.00004$, in agreement with our experimental observation that the c_{pc} lattice constant is weakly dependent on thickness. Finally, the computed polarization is very weakly affected by the uth-to-th transition: We obtained $P=88\ \mu\mathrm{C/cm}^2$, with in-plane and

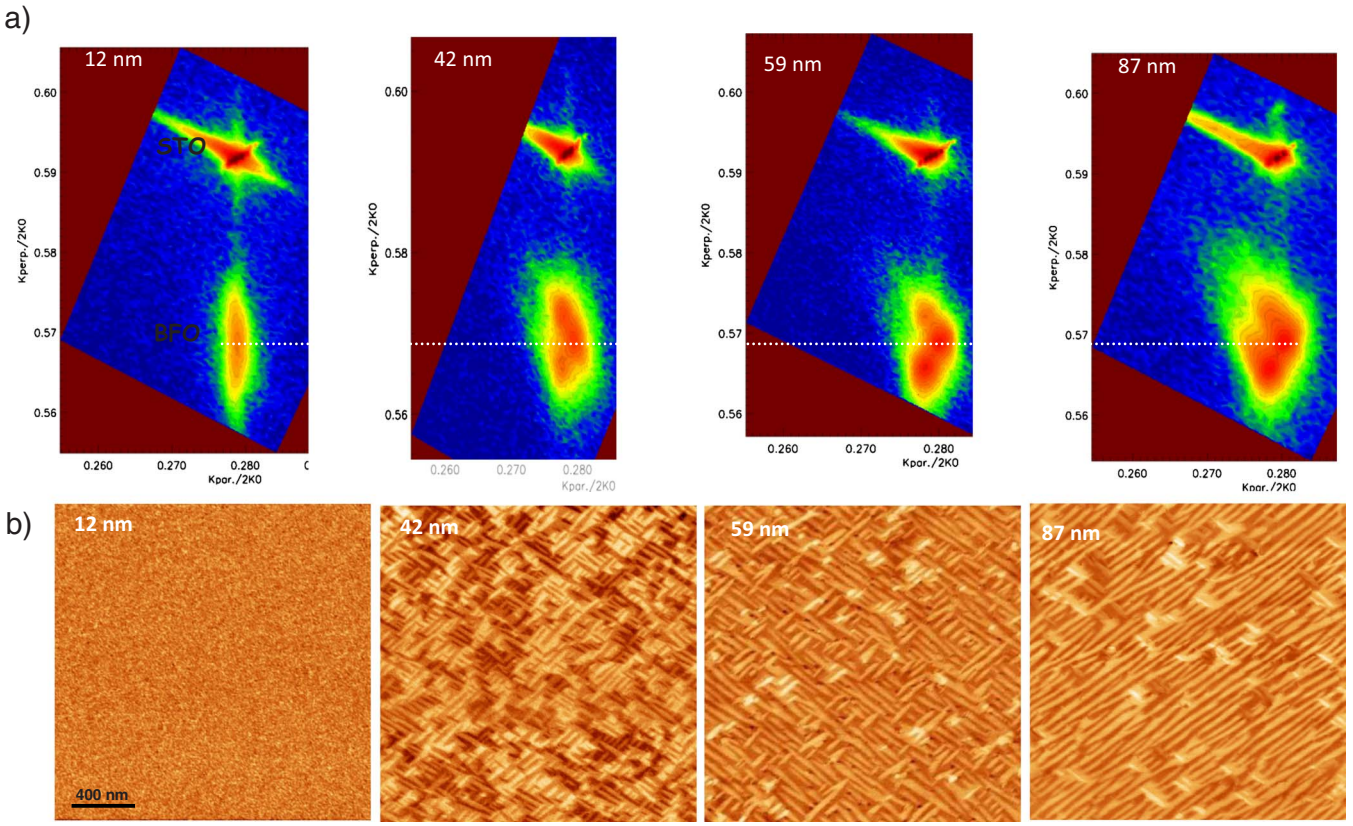

FIG. 2. (Color online) (a) Reciprocal space maps around the $(103)_m$[=$(113)_{pc}$] reflections for different thicknesses of the BFO films. The axes are in units of $2k_o=4\pi/\lambda$, with $\lambda=1.5405$ Å. The horizontal line through the maps indicates the out-of-plane reciprocal lattice spacing, which is unchanged in the range of studied thicknesses. (b) In-plane piezoresponse images of the same films.

out-of-plane components of 66 and 58 $\mu C/cm^2$, respectively. The polarization forms an angle of about 5.1° with the body diagonal of the pseudocubic cell, being rotated toward the [001] direction.

The observed c_{pc}/a_{pc} aspect ratio of our BFO films deserves one additional comment. In the course of this study, wanting to investigate the relationship between the value of c_{pc}/a_{pc} and the out-of-plane polarization, we simulated the hypothetical case of a strained BFO film forced to be in a centrosymmetric (paraelectric) structure but allowing for the O_6 rotations; we obtained a c_{pc}/a_{pc} of about 1.04, a result that is similar to the one mentioned above for the polarized case and compatible with our experimental data. (Interestingly, if the O_6 rotations are also artificially suppressed, which corresponds to a fully symmetric strained film with the $P4/mmm$ space group, the computed c_{pc}/a_{pc} drops to 1.02.) Note that this lack of correlation between c_{pc}/a_{pc} and the magnitude of the polar distortion constitutes an important difference between BFO and traditional ferroelectrics such as $PbTiO_3$ or PZT. Indeed, our results suggest that in the case of BFO one should avoid using crystallographic information about the (tetragonally distorted) unit cell as proof for a polar state; direct evidence for the polarization (e.g., as provided by our piezoresponse measurements) is mandatory.

Let us now describe the evolution of the domain structure. Analysis of the RSMs in Fig. 2 shows that the domain walls that prevail are the 71° ones [see Fig. 1(c)] in agreement with previous reports.[18] We have been able to understand why.

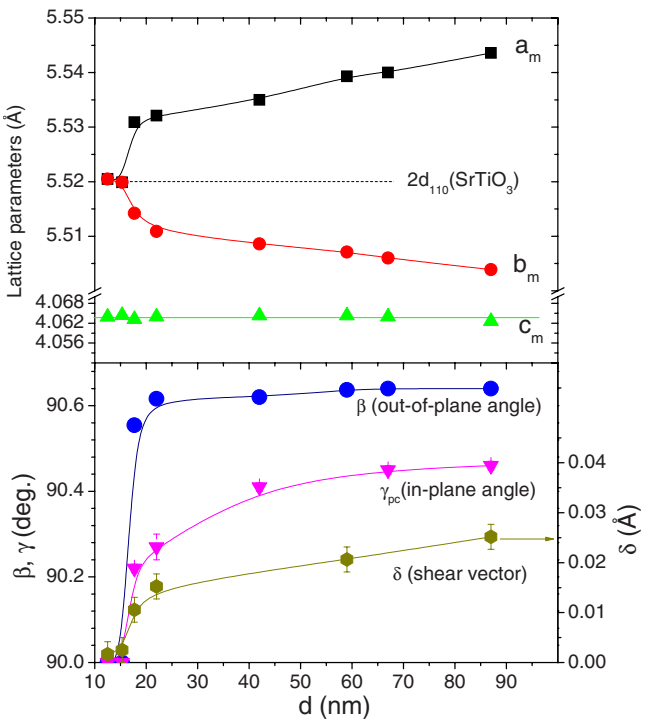

FIG. 3. (Color online) Evolution of monoclinic lattice parameters and shear displacement as a function of thickness.

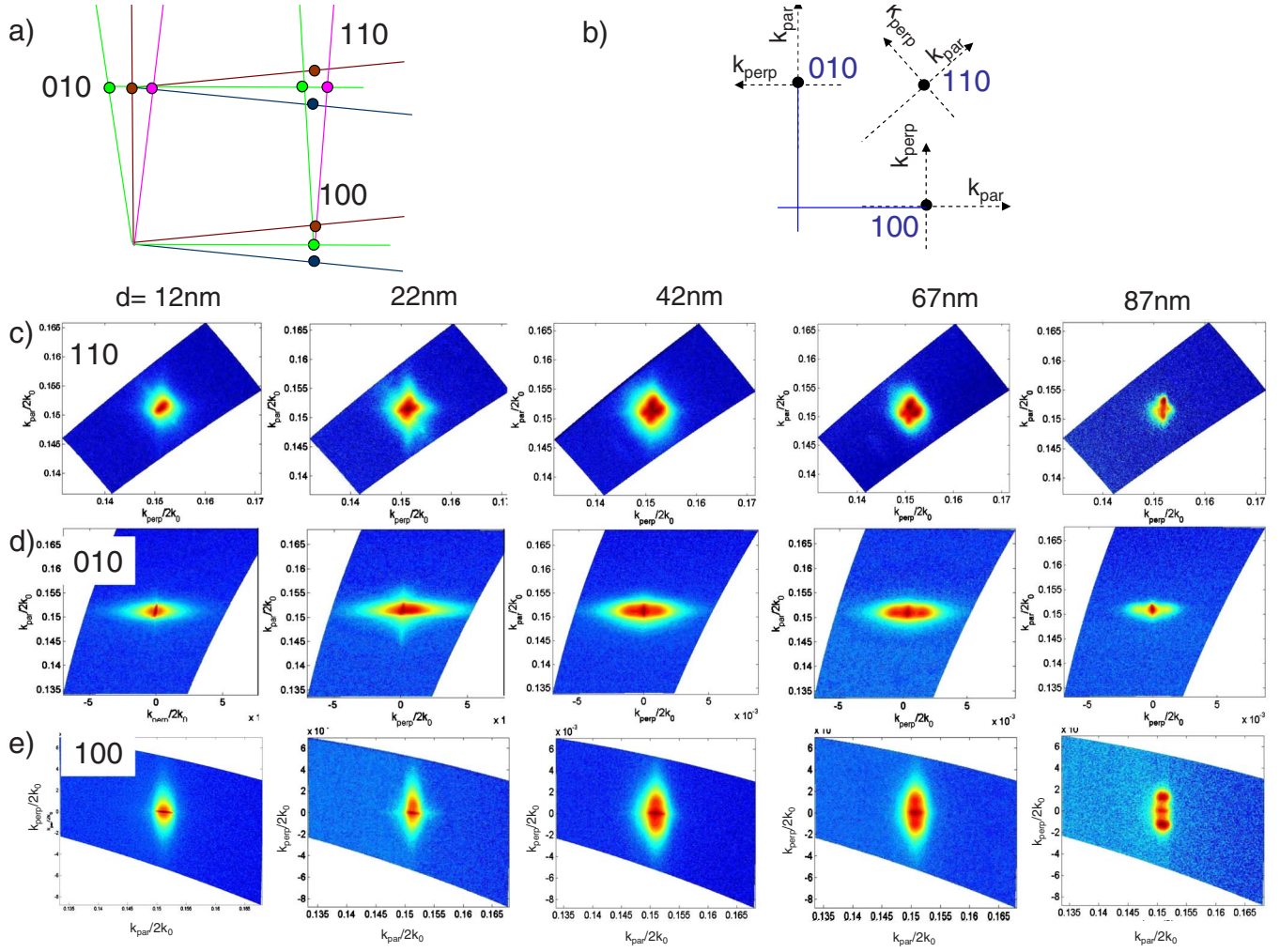

FIG. 4. (Color online) (a) Sketch of the RSM's expected around the (100), (010), and (110) pseudocubic reflections when all four domains are present; (b) directions of k_{par} and k_{perp} in each case; [(c)–(e)] maps around (110), (010), and (100), respectively, for different film's thicknesses. The axes are in units of $2k_o$, where $k_o = 2\pi/\lambda$.

This is confirmed by PFM imaging [Fig. 2(b)] as well as by grazing incidence diffraction (Fig. 4). Out-of-plane PFM measurements show that all the films are polarized down, also in agreement with previous reports.[18] In Fig. 2(b), in-plane PFM (IP-PFM) images of the same films are shown. In agreement with the XRD data, we observe a clear evolution of the domain pattern. For the thinnest films, no contrast is detected on the IP-PFM images. IP-PFM images for intermediate films show a clear stripelike pattern. These stripes indicate four polarization variants, which are in good agreement with rhombohedral-like monoclinic distortions[19] [see Fig. 1(c)] and with the RSM maps. We observe that the number of variants decreases from four to two variants with further increasing thickness, allowing for longer stripes for the thicker films.

Mapping of the in-plane reciprocal space has also been performed and the main results are shown in Fig. 4. In Fig. 4(a) we sketch the expected reflections around the (110), (010), and (100) reciprocal lattice points when the four domains are present. Maps around these directions are shown in Figs. 4(c)–4(e), respectively, for films with different thicknesses. The directions of the parallel and perpendicular components of the scattering vector in each case are shown in Fig. 4(b). These measurements confirm the domain evolutions previously described: the 12-nm-thick films are fully coherent; for thicknesses larger than about 18 nm, four domains variants appear; finally, for the 87-nm film, we see that two of the four variants are preferred. Several works have already shown two-variant stripe domains for (001)-oriented BFO films, by using high miscut STO substrates[12,20] or orthorhombic substrates.[21] The origin of this reduction in polarization orientations in BFO films was reported to be the step-flow growth and the substrate anisotropy, respectively. Since the growth mode as well as the substrate miscut in all our films are the same, our results point to yet a different mechanism.

All this evidence fits a simple but powerful model by which the domain formation enables and controls the monoclinic distortion of the unit cell. Figure 5(a) shows how twinning reduces the in-plane strain introduced by the pseudocubic angle, γ_{pc} (characteristic of the monoclinic distortion). Two pairs of twins, coherent along [100] (v_1) or along [010] (v_2), can form. It can also be seen that, in order to do that, the in-plane lattice parameters of the film, a_f and b_f, deviate

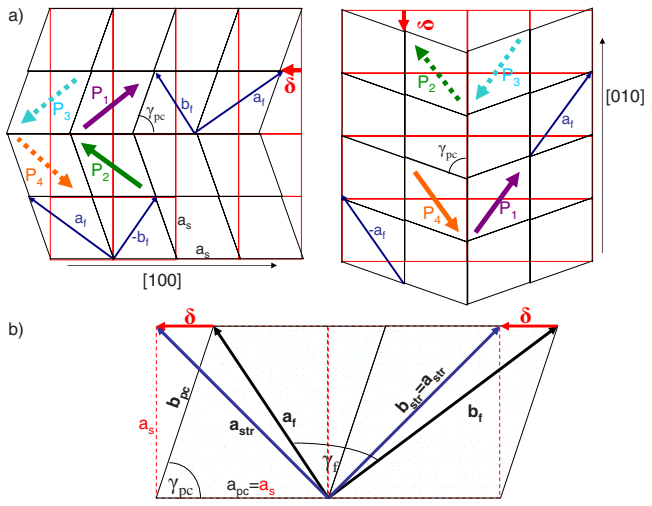

FIG. 5. (Color online) (a) The two types of twins present in the films, each including 71° walls: v_1 (left) is coherent along [100] and v_2 (right) is coherent along [010]. (b) Detail of the film distortion.

equally from the fully strained values of $a_{srt}=b_{str}=\sqrt{2}a_{\mathrm{STO}}$, i.e., $\vec{a}_f=\vec{a}_{str}-\vec{\delta}$ and $\vec{b}_f=\vec{b}_{str}-\vec{\delta}$, as sketched in Fig. 5(b). The magnitude of the shear vector $\vec{\delta}$, therefore, determines both a_f and b_f, which split *symmetrically* with increasing thickness, excellently explaining our experimental observations (see Fig. 3). As a result, the in-plane area of the film is unchanged with respect to the fully coherent film, which in turn seems compatible with the observation that the c_m lattice parameter does not vary during strain relaxation (for thicknesses up to 100 nm). A more subtle result of this relaxation process is that the symmetry of the film unit cell is actually lower than monoclinic; indeed, it can be seen from Fig. 4(b) that the angle between $\vec{a}_f$ and $\vec{b}_f$ is given by $\gamma_f=\cos^{-1}(\delta^2/a_f b_f)$, and thus different from 90°. A very similar twinning mechanism with symmetry lowering has been found in thin films of $TbMnO_3$ grown on (001)-STO substrates,[22] which suggests it may be typical of low-symmetry perovskites on cubic substrates.

As observed in Fig. 5(a), the two pairs of variants, 90° rotated from each other, are in agreement with the PFM maps of the 42- and 59-nm films and give rise to both 71° and 109° walls. Even though both nucleate with equal probability in the growing film, on a low-miscut substrate, because of the relatively large-strain energy store at the boundary between them, for thicker films (and therefore larger strain energy at those boundaries) one of the two variants will be preferred, as observed in the thicker 87-nm film, and mostly 71° walls remain. In the presence of a substrate miscut, the steps can indeed determine which of the two variant is present[12] but this will also happen in exact substrates provided that the films have enough time to relax. These 71° walls can be atomically perfect and defect-free (see Fig. 5). This may explain the more insulating nature of the 71° walls of $BiFeO_3$, as compared with the 109° and 180° walls.[10]

It is worth mentioning that the domain orientations observed here, after slow PLD growth, have rarely been reported so far[4] and that, typically, more complex reciprocal space maps than those in Fig. 2 are observed around the $(h0l)_m$ reflections.[5,12,23] The reason for that is that most of the films reported contain domains that have crystal orientations with out of plane tilts and, thus, do not share the pseudocubic [001] direction with the substrate.[23] However, the lack of a coherent interface can, in some cases, be advantageous since these films are less clamped and could better allow polarization rotation[7] or a lower leakage characteristics.[23,24] These differences are determined not only by the substrate miscut but also by the growth conditions. Here we show that it is possible to control not only the structure and the type of domains but also their orientation relative to the substrate, which is of crucial importance to understand the ferroelectric properties of the films.

IV. SUMMARY

We have observed clear trends in the evolution with thickness of the structure and microstructure of $BiFeO_3$ films on (001)-$SrTiO_3$ substrates. We have shown that the lattice parameters and the film symmetry do not result simply from the mismatch with the substrate but also from the occurrence of a particular twinning that allows for the observed monoclinic distortion. Such an effect provides us with a new degree of freedom for tuning the structural and physical properties of the thin films. This twinning model explains why the 71° domain walls are so often observed in atomically flat films on (001)-$SrTiO_3$. Our results suggest that the physics behind the effects of epitaxial strain is richer than usually thought, and that traditional thermodynamic phase diagrams and first-principles models need to be complemented with knowledge of the domain structure in order to reach a full understanding of the materials behavior.

ACKNOWLEDGMENTS

We are grateful to Gijsbert Rispens and Sriram Venkatesan for useful discussions and to Wolfgang Caliebe for his help at the W1 beamline. This work was partly funded by MaCoMuFi (Grant No. STREP_FP6-03321), the Spanish DGI (Grants No. FIS2009-12721-C04-03 and No. CSD2007-00041) and the Dutch agencies NWO and FOM. We made use of the facilities of the BSC-CNS and CESGA supercomputing centers.

*Corresponding author; b.noheda@rug.nl

[1] R. Ramesh and N. A. Spaldin, Nature Mater. **6**, 21 (2007).
[2] J. Wang, J. B. Neaton, H. Zheng, V. Nagarajan, S. B. Ogale, B. Liu, D. Viehland, V. Vaithyanathan, D. G. Schlom, U. V. Waghmare, N. A. Spaldin, K. M. Rabe, M. Wuttig, and R. Ramesh, Science **299**, 1719 (2003).
[3] G. Catalan and J. F. Scott, Adv. Mater. **21**, 2463 (2009); G. Catalan, H. Bea, S. Fusil, M. Bibes, P. Paruch, A. Barthelemy, and J. F. Scott, Phys. Rev. Lett. **100**, 027602 (2008).
[4] G. Xu, H. Hiraka, G. Shirane, J. Li, J. Wang, and D. Viehland, Appl. Phys. Lett. **86**, 182905 (2005).
[5] H. Bea, M. Bibes, S. Petit, J. Kreisel, and A. Barthelemy, Philos. Mag. Lett. **87**, 165 (2007).
[6] D. H. Kim, H. N. Lee, M. D. Biegalski, and H. M. Christen, Appl. Phys. Lett. **92**, 012911 (2008).
[7] H. W. Jang, S. H. Baek, D. Ortiz, C. M. Folkman, R. R. Das, Y. H. Chu, P. Shafer, J. X. Zhang, S. Choudhury, V. Vaithyanathan, Y. B. Chen, D. A. Felker, M. D. Biegalski, M. S. Rzchowski, X. Q. Pan, D. G. Schlom, L. Q. Chen, R. Ramesh, and C. B. Eom, Phys. Rev. Lett. **101**, 107602 (2008).
[8] B. Noheda, D. E. Cox, G. Shirane, J. A. Gonzalo, L. E. Cross, and S. E. Park, Appl. Phys. Lett. **74**, 2059 (1999).
[9] L. Bellaiche, A. Garcia, and D. Vanderbilt, Phys. Rev. Lett. **84**, 5427 (2000).
[10] J. Seidel, L. W. Martin, Q. He, Q. Zhan, Y. H. Chu, A. Rother, M. E. Hawkridge, P. Maksymovych, P. Yu, M. Gajek, N. Balke, S. V. Kalinin, S. Gemming, F. Wang, G. Catalan, J. F. Scott, N. A. Spaldin, J. Orenstein, and R. Ramesh, Nature Mater. **8**, 229 (2009).
[11] L. W. Martin, Y. H. Chu, M. B. Holcomb, M. Huijben, P. Yu, S. J. Han, D. Lee, S. X. Wang, and R. Ramesh, Nano Lett. **8**, 2050 (2008).
[12] H. W. Jang, D. Ortiz, S.-H. Baek, C. M. Folkman, R. R. Das, P. Shafer, Y. Chen, C. T. Nelson, X. Pan, R. Ramesh, and C.-B. Eom, Adv. Mater. **21**, 817 (2009).
[13] M. Alexe and A. Gruverman, *Nanoscale Characterization of Ferroelectric Materials* (Springer-Verlag, Berlin, 2004).
[14] B. Noheda, D. E. Cox, G. Shirane, S.-E. Park, L. E. Cross, and Z. Zhong, Phys. Rev. Lett. **86**, 3891 (2001).
[15] The indexes are with respect to the *Cm* space group, as in Ref. 14. With XRD we are not sensitive to oxygen rotations as thus we cannot distinguish between *Cc* and *Cm*.
[16] O. E. González-Vázquez and J. Íñiguez, Phys. Rev. B **79**, 064102 (2009).
[17] A. J. Hatt, N. A. Spaldin, and C. Ederer, Phys. Rev. B **81**, 054109 (2010).
[18] Y. H. Chu, T. Zhao, M. P. Cruz, Q. Zhan, P. L. Yang, L. W. Martin, M. Huijben, C. H. Yang, F. Zavaliche, H. Zheng, and R. Ramesh, Appl. Phys. Lett. **90**, 252906 (2007).
[19] F. Zavaliche, S. Y. Yang, T. Zhao, Y. H. Chu, M. P. Cruz, C. B. Eom, and R. Ramesh, Phase Transitions **79**, 991 (2006).
[20] R. R. Das, D. M. Kim, S. H. Baek, C. B. Eom, F. Zavaliche, S. Y. Yang, R. Ramesh, Y. B. Chen, and X. Q. Pan, Appl. Phys. Lett. **88**, 242904 (2006).
[21] Y. H. Chu, Q. Zhan, L. W. Martin, M. P. Cruz, P. L. Yang, G. W. Pabst, F. Zavaliche, S. Y. Yang, J. X. Zhang, L. Q. Chen, D. G. Schlom, T. B. Wu, and R. Ramesh, Adv. Mater. **18**, 2307 (2006).
[22] S. Venkatesan, C. J. M. Daumont, B. J. Kooi, B. Noheda, and J. Th. M. De Hosson, Phys. Rev. B **80**, 214111 (2009); C. J. M. Daumont, D. Mannix, S. Venkatesan, G. Catalan, D. Rubi, B. J. Kooi, J. Th. M. De Hosson, and B. Noheda, J. Phys.: Condens. Matter **21**, 182001 (2009).
[23] H. Liu, P. Yang, K. Yao, and J. Wang, Appl. Phys. Lett. **96**, 012901 (2010).
[24] L. Pintilie, C. Dragoi, Y. H. Chu, L. W. Martin, R. Ramesh, and M. Alexe, Appl. Phys. Lett. **94**, 232902 (2009).